Sectional and Overall Reachability for Systems with S-Shaped Distillation Lines

Warren R. Hoffmaster and Steinar Hauan
Dept. of Chemical Engineering, Carnegie Mellon University, Pittsburgh, PA 15213

Total and minimum reflux bounds serve as limiting case scenarios for determining feasibility in azeotropic distillation columns. Specifically, all reachable feed compositions in a staged rectifying or stripping section have been reported as the union of points enclosed by the distillation and pinch-point curves through a desired product. By eigenvalue considerations of pinch bifurcations and geometric analysis of fundamental region structures, the region of all reachable compositions has seemingly been identified. Additional insights are needed to fully characterize the feasible compositions in a subset of azeotropic mixtures. This article describes how sectional profiles can actually cross pinch-point curves and generate a region of additional feasibility outside the one previously reported. It also demonstrates how a substantially larger region between the distillation line and pinch-point curve after the intersection is only accessible by composition profiles going through the extended region. This extended reachable region is explained by evaluating the conditions for a fixed point in composition space. The effect on sectional profiles is illustrated for both an artificially parametric VLE manifold and a nonideal azeotropic system with more than one simple distillation region. Sectional profiles extended beyond the traditional bounds affect coupled sections in a distillation cascade.

Introduction

The preliminary step in process design is identifying types of equipment that might achieve a set of desired objectives. It is important that a complete list of alternative structures is identified in the synthesis step to ensure that all possible process configurations are considered for the final design. With this exhaustive set of alternatives in hand, each structure is then evaluated in terms of feasibility. This step asks whether a particular process configuration can meet the design goals (that is, product specifications). The intent of a feasibility check is to quickly establish, without carrying out a detailed design, whether or not a process alternative has the capability to perform the desired task. Once the set of structures is narrowed down to a few feasible alternatives, a more in-depth design is necessary to determine which structure is most suitable in terms of economics, process control, and operability.

Significant research efforts have focused on developing process synthesis methods and feasibility criteria for distillation systems. Westerberg and Wahnschaft (1996) review column sequencing algorithms that have been established for separating multicomponent ideal mixtures. Synthesis tools for systems exhibiting azeotropic behavior are largely based on the thermodynamic topological analysis (Serafimov, 1987; Hilmen, 2000) described in the Russian literature. Although this geometric approach has been generalized for n-component systems, most research efforts toward a systematic synthesis method for azeotropic mixtures have been confined to ternary systems.

Feasibility conditions for distillation are based on the two extreme operating conditions for a continuous distillation process—minimum and total reflux. Neither condition is practical for operating a distillation column, because an infinite number of stages and intermediate condensers and reboilers are required for minimum reflux while no product is withdrawn at total reflux. However, these limiting conditions traditionally serve as bounds for distillation. Based on these extreme operation limits, graphical approaches have been developed to determine where in composition space a column can operate. These methods divide the column into sections (rectifying and stripping) in which column pressure is fixed

Correspondence concerning this article should be addressed to S. Hauan.

and all stages are theoretical. Generally, it is also assumed that constant molar overflow (CMO) exists in each section, but this restriction can readily be lifted if heat effects are considered.

Using the extreme operating conditions, feasibility criteria have been developed for two different column-design approaches. The most common technique specifies the feed composition and determines all reachable products (Wahnschafft et al., 1992; Fidkowski et al., 1993; Westerberg and Wahnschafft, 1996). The other approach, which has received more attention lately, identifies all feed compositions that will produce a specified product when fed to a column section (Pöllmann and Blass, 1994; Westerberg and Wahnschafft, 1996; Castillo et al., 1998).

These techniques will reliably determine column feasibility as long as all reachable compositions are contained between the minimum and total reflux bounds. However, it has been noted (Castillo et al., 1998) that sectional profiles for columns can extend beyond these extreme operating limits in regions of composition space where the total reflux curves (distillation lines for a staged column and residue curves for a packed column) take on an S-shape. The additional reachable region has been neglected because it is thought of as being relatively small compared to the enclosed area found from traditional reachability. Since S-shaped total reflux curves are common in azeotropic systems, the effect of these regions on reachability must be fully characterized before reachable regions are used as a sufficient criterion for feasibility.

The aim of this work is to identify and verify the existence of an extended reachable region for separating certain multicomponent azeotropic systems due to the presence of S-shaped total reflux curves. We will also study the effects that S-shaped curves have on column feasibility.

Fundamentals of Sectional Reachability

An algorithm has been proposed by Castillo et al. (1998) to evaluate column feasibility for homogeneous azeotropic systems. This procedure is based on the principle of finding all feed compositions that will produce a specified product in a column section. The region encompassing all possible feeds or column section profiles is termed the operation leaf or reachable region. Once the reachable regions are constructed for both the rectifying and stripping sections, a separation can quickly be deemed feasible if the regions overlap one another. The only necessary assumption is a fixed column pressure, but for reasons of simplicity we will also assume CMO and equilibrium stages. It should be noted that one key limitation of this approach is that only ternary systems have been considered so far.

The method to construct the reachable regions for a single-feed column with two products is as follows:

Step 1. Specify the Column Pressure, Distillate Composition, and Bottoms Composition. When the column pressure is fixed, a mixture can be classified in terms of thermodynamic and topological features of the vapor–liquid equilibrium manifold. The distinguishing characteristics such as azeotropes and distillation boundaries also provide insights for specifying top and bottom product compositions.

Step 2. Construct the Total Reflux Bounds. A total reflux curve is drawn in the direction of increasing (decreasing) temperature from the specified distillate (bottoms) composition. The curves are continued until a pure component or binary azeotrope is reached. Distillation lines (Stichlmair, 1988) represent total reflux for staged columns, while residue curves (Doherty and Perkins, 1978) approximate this condition for packed columns.

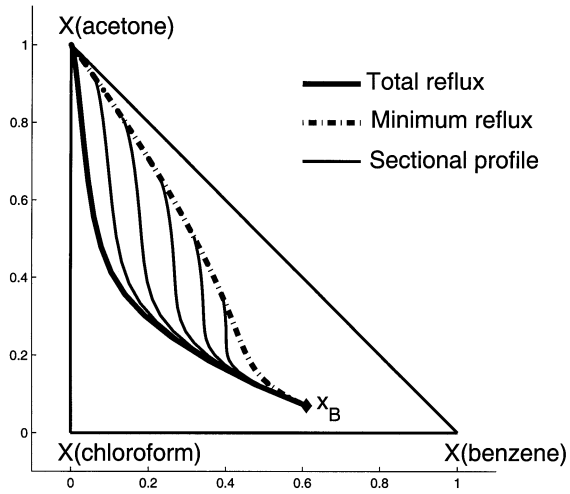

Figure 1. Closed reachable region.

Step 3. Construct the Minimum Reflux Bounds. Pinch-point curves (Wahnschafft et al., 1992) describe the minimum reflux condition. A pinch point occurs when the vector between liquid (x) and vapor (y) equilibrium compositions is colinear to the material balance line. Like the total reflux bounds, the pinch-point curve is continued from the specified distillate (bottoms) composition in the direction of increasing (decreasing) temperature until an edge of the composition space is reached. Azeotropic mixtures often have multiple pinch-point curves that have been shown to bifurcate. These curves can be accurately computed using the colinearity condition along with bifurcation/continuation software such as Auto97 (Doedel, 1998).

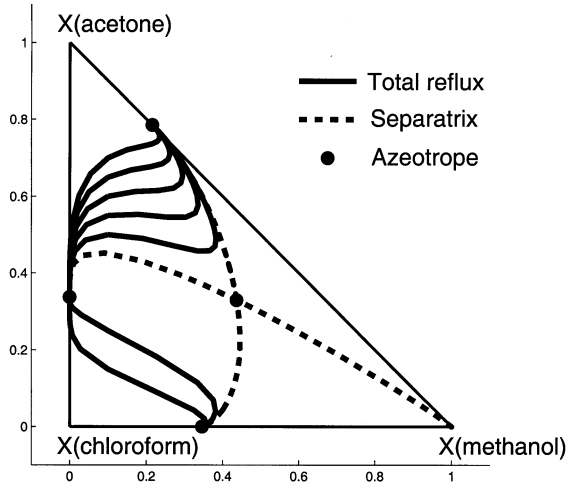

Figure 2. S-shaped distillation lines.

The total reflux bounds and pinch-point curves for both column sections are plotted in composition space. Generally, the liquid compositions are used to represent the reachable regions. For most specified product compositions, the distillation line and pinch-point curve through the product will end at the same point, creating a closed region between the two curves. An example, closed reachable region for a specified bottoms product, is presented in Figure 1 for a mixture of acetone, chloroform, and benzene. Sectional profiles for the full range of reboil ratios are all contained in the enclosed area.

However, in some instances, the total reflux bound and pinch-point curve diverge from each other. This occurs when the specified product is placed close to a distillation boundary. Under these circumstances, certain sectional profiles at finite reflux cross the boundary (Van Dongen, 1983; Wahnschafft, 1992; Wahnschafft et al., 1992). The reachable region can still be established, but the bounds on the region will now include an edge of composition space in addition to the multiple pinch-point curve branches and the total reflux bound. The term open operation leaf (Castillo et al., 1998) is given to these modified operating bounds.

Another interesting and not fully understood exception to the traditional reachable region occurs when the total reflux curves take on an S shape. The following section examines the impact of S-shaped distillation lines on sectional reachability.

New Insights on S-Shaped Distillation Lines

Identification of S-shaped distillation lines

The acetone–chloroform–methanol mixture in Figure 2 has three binary and one ternary azeotrope, all connected by distillation boundaries. In the uppermost region, distillation lines begin at the acetone–methanol azeotrope (328 K) and terminate at the acetone–chloroform azeotrope (338 K). Distillation lines in the lower left region head from the chloroform–methanol azeotrope (327 K) to the acetone–chloroform azeotrope. Acetone (329 K), chloroform (334 K), and the ternary azeotrope (330 K) are intermediate boilers. Total reflux curves in the other two regions terminate at methanol (338 K).

The distillation lines drawn in Figure 2 are S-shaped, which is common in many azeotropic mixtures. The S shape in these curves reflects the presence of inflection points. This feature easily can be used to detect regions of composition space with S-shaped distillation lines.

Inflection points are found by first characterizing the VLE in terms of unidistribution ($K_i = 1$) and univolatility ($\alpha_{i,j} = 1$) lines. These lines, which can be detected directly from a phase equilibrium relationship, provide important information about the pathways of total reflux curves (Hilmen, 2000; Kiva and Serafimov, 1973). When a system contains no univolatility lines, the distillation lines have no inflection points, ruling out the possibility of S-shaped curves. Univolatility lines, by themselves, do not guarantee inflection points, but they must be present in order for inflection points to exist. There are two scenarios that give rise to inflection points along the distillation lines. The first condition says that a distillation line has an inflection point if the distillation line does not cross any K_i or K_j unidistribution lines as it runs from a particular

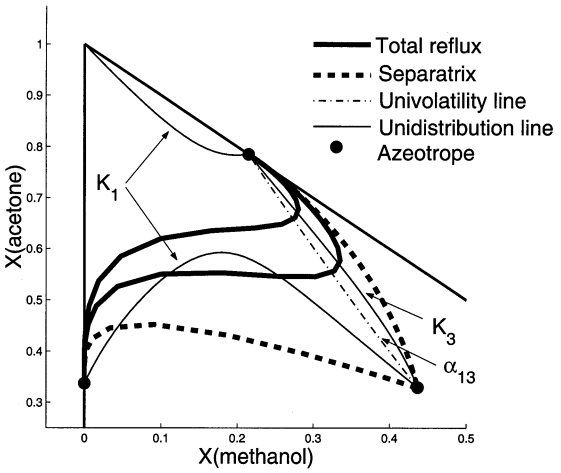

Figure 3. Characterization of VLE using unidistribution and univolatility lines.

univolatility line ($\alpha_{i,j} = 1$) to either a stable or unstable node. To apply this condition, each univolatility line must be checked individually to detect all areas of composition space where inflection points exist. The second condition has two parts based on the same concept. The first part states that a distillation line has an inflection point if it intersects the unidistribution line(s) of one component twice in succession. Similarly, the other part of the second condition says that an inflection point exists along a distillation line if it intersects any univolatility line(s) with the same indices twice in a row.

These conditions will be illustrated using the acetone–chloroform–methanol system shown in Figure 2. The unidistribution and univolatility lines, along with two S-shaped distillation lines, are constructed in Figure 3 for the uppermost distillation region. To begin, the uppermost total reflux curve will be analyzed to determine why it is S-shaped. The first condition is applied by studying the behavior of this distillation line as it heads away from the $\alpha_{13} = 1$ line. Following this distillation line to the left toward the stable

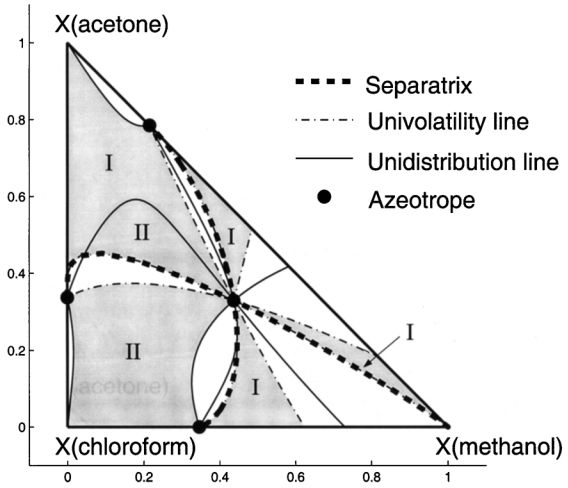

Figure 4. Regions of composition space with S-shaped distillation lines.

acetone–chloroform binary azeotrope, no K_1 or K_3 unidistribution lines are crossed, indicating the presence of an inflection point. On the other side of the $\alpha_{13}=1$ line, this distillation line heads in the direction of the unstable acetone–methanol node and crosses the $K_3=1$ line, eliminating the possibility of having any inflection points on the right side of the univolatility line. The inflection point to the left of the univolatility line results in the S-shaped behavior.

The lower total reflux curve in Figure 3 exhibits different characteristics despite having the same S-shape as the distillation line previously studied. According to the first condition, this distillation line has no inflection points to the left of the α_{13} univolatility line because the K_1 unidistribution line is crossed. The first condition is also violated to the right of the $\alpha_{13}=1$ line since the distillation line intersects the $K_3=1$ line. However, the second criterion for identifying inflection points becomes relevant in this case. To the left of the $\alpha_{13}=1$ line, the distillation line intersects the $K_1=1$ line twice successively, which explains why an inflection point exists.

This method can be used to completely map out regions of composition space where S shapes exist. A full analysis of the acetone–chloroform–methanol mixture yields six distinct regions (Figure 4) where S shapes are possible along the distillation lines. The four shaded regions labeled "I" have inflection points according to the first condition, while the other two shaded areas labeled "II" have inflection points as a result of the second condition. The same rules apply for finding inflection points for packed columns described by residue curves. With an understanding of when S-shaped distillation lines occur, we will now take a closer look at the effect of S shapes on reachable regions.

Reachability with S-shaped distillation lines

In regions of composition space where the distillation lines are S-shaped, sectional profiles can cross outside the region contained between the minimum and total reflux bounds before reaching stationary points. Figure 5 shows an enlarged picture of one of the S-shaped distillation lines in the uppermost distillation region of the acetone–chloroform–methanol mixture. The bottoms product is placed close to the inflection point, and the traditional feed regions are constructed. Due to the presence of the S shape in the distillation line, the reachable region consists of two enclosed areas. Based on traditional reachability, both regions would be considered feasible. As expected, the sectional profile for a small reboil ratio ($s=1$) is completely contained by the pinch-point curve and distillation line. Larger reboil ratios, however, cause the profiles to begin in one enclosed region and cross outside the bounds before returning to the other closed area. Crossing profiles exit the first reachable region through the pinch-point curve and then reenter the other region through the distillation line. Once a sectional profile that crosses the traditional bounds is found, all higher reboil ratios will lead to crossing profiles. This behavior results in an additional area of reachability that must be captured. Before developing methods to bound this additional reachable region, we will try to better understand why this extended region exists.

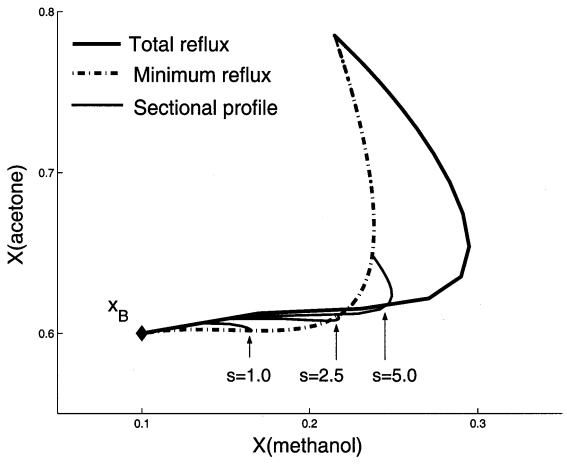

Figure 5. Sectional profiles in an S-shaped region (stripping section).

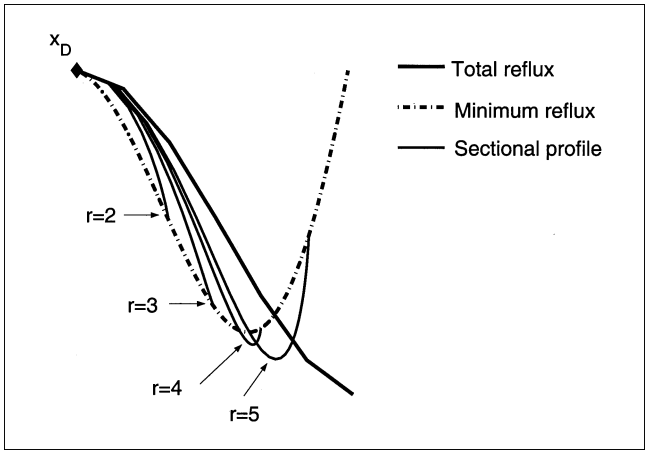

Figure 6. Sectional profiles crossing the pinch-point curve for parametric VLE.

Verification of extended reachable region using parametric VLE

To eliminate any dependency on VLE model parameters, parametrically generated vapor–liquid equilibrium data are used to reconstruct the situation in which sectional profiles cross the pinch-point curve. Sine curves serve to reproduce the S shapes in the total reflux bounds. Discrete points along the sine curve represent equilibrium stages for distillation lines, while the continuous sine function depicts residue curves. Pinch points are then determined based on the colinearity condition, which requires the liquid ($\boldsymbol{x}$) and vapor ($\boldsymbol{y}$) leaving a stage to lie along the same line as the specified end-product for the column section. When the tangent to the residue curve (the $\boldsymbol{x}-\boldsymbol{y}$ vector) is colinear to the specified product composition, the necessary pinch condition has been satisfied. The locus of pinch points for the full range of reflux or reboil ratios constitutes the pinch-point curve. It is important to realize that pinch-point curves are the same for both packed and staged column sections despite the fact that residue curves are used to detect pinch points. With an un-

derstanding of the traditional reachability bounds for the parametric VLE, feasibility bounds and sectional profiles based on artificial VLE are constructed in Figure 6 for a rectifying section, producing the specified distillate composition. Due to the S shape in the distillation line, the minimum and total reflux curves intersect and create two separate regions where sectional profiles would be expected to stay contained. Low reflux ratios ($r \leq 3$) keep the sectional profiles in the first region; however, larger reflux ratios cause profiles to cross through the pinch-point curve. This behavior is the same as that seen in the real system (Figure 5) and confirms that an extended region of reachability exists when column section end-products lie along S-shaped distillation lines. From the use of parametric VLE, it is clear that this behavior is a geometric feature of equilibrium step sequences.

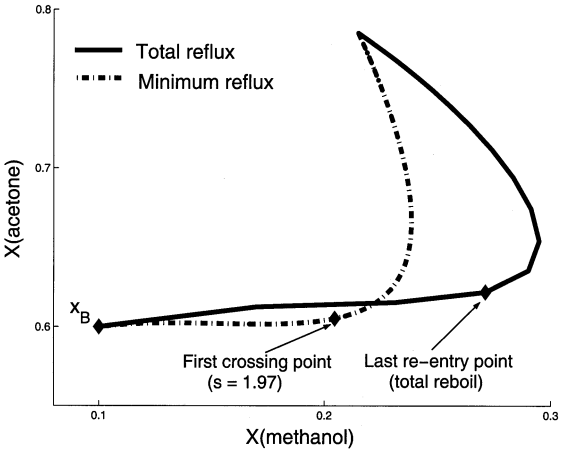

Figure 8. Location of extended region.

Explanation of the pinch-point curve crossing

To understand why sectional profiles cross the pinch-point curve in regions of composition space with S-shaped distillation lines, we need to study the geometry associated with pinch points. For a stripping section, the geometry around a pinch point is presented in Figure 7a. From the liquid composition leaving stage n ($\boldsymbol{x}_n$), the stage-to-stage calculations proceed by taking an equilibrium step to find the corresponding vapor composition ($\boldsymbol{y}_n$). We next determine where the liquid leaving stage $n+1$ ($\boldsymbol{x}_{n+1}$) lies in composition space. The material balance forces $\boldsymbol{x}_{n+1}$ to be colinear with both $\boldsymbol{y}_n$ and the specified product ($\boldsymbol{x}_B$). The relative placement of $\boldsymbol{x}_{n+1}$ along the mass-balance line is determined by the reboil ratio. This column section pinches because the material balance returns the liquid composition to $\boldsymbol{x}_n$, creating a cycle in which stage-to-stage compositions remain unchanged.

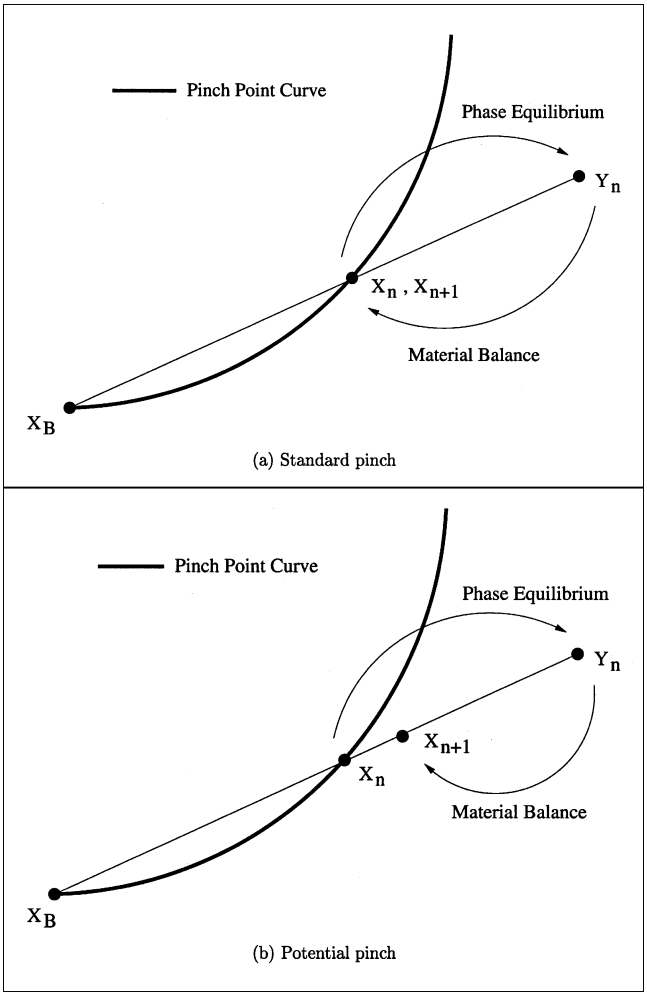

Figure 7. Geometric view of a pinch point.

In the case of S-shaped distillation lines, the pinch geometry is studied at a point along the pinch-point curve at which sectional profiles cross outside the minimum reflux bound. For the potential pinch point $\boldsymbol{x}_n$ in Figure 7b, the phase-equilibrium step determines the location of $\boldsymbol{y}_n$. However, for the specified reboil ratio, we find that $\boldsymbol{x}_{n+1}$ does not fall at the same point as $\boldsymbol{x}_n$, thus, not giving rise to a pinch point at this reboil ratio. Even though the phase equilibrium and material balance cause the liquid and vapor leaving stage n to be colinear, there is a length mismatch preventing the two vectors from canceling each other. A different reboil ratio would be needed to make the column section pinch at $\boldsymbol{x}_n$. Actual pinch points must not only satisfy the colinearity condition but must also have equal-length material balance and phase-equilibrium vectors pointing in opposite directions.

Pinch-point curves are tracked using the colinearity condition so all possible points satisfying this criteria are found. Each pinch point has a single reflux ratio associated with it that will cause a sectional profile drawn with that reflux to terminate. If a sectional profile reaches a point on the pinch-point curve with a different reflux ratio than the one associated with the pinch point, the profile will continue on until a pinch point with the proper reflux ratio is reached. In the case of ideal systems, column profiles always reach pinch points with the proper reflux ratio. However, sectional profiles in systems with S-shaped distillation lines often reach points with an incorrect reflux ratio. This causes the profile to cross through the pinch-point curve and head to another pinch point with the right reflux. We will use this idea of pinch-point stability in the next section to develop methods for detecting the extended region.

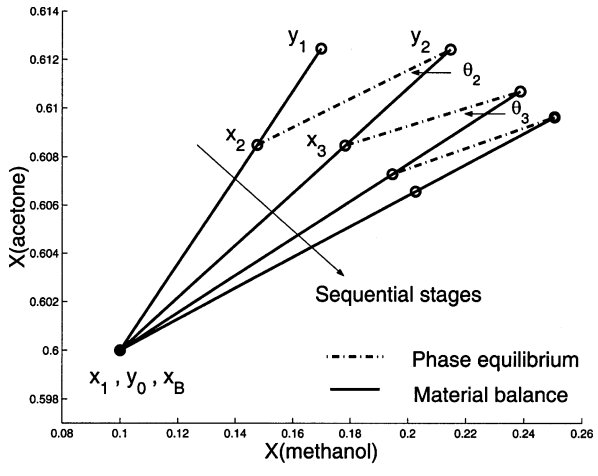

(a) Stage-to-stage calculations

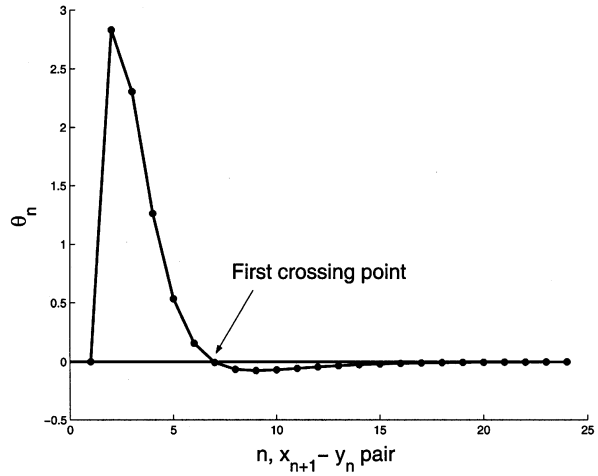

(b) Angle for sequential stages

Figure 9. Determining pinch-point curve crossing using angle criteria.

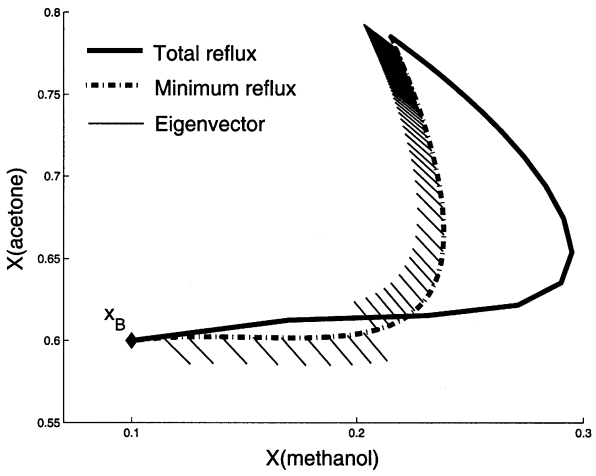

(a) Eigenvectors

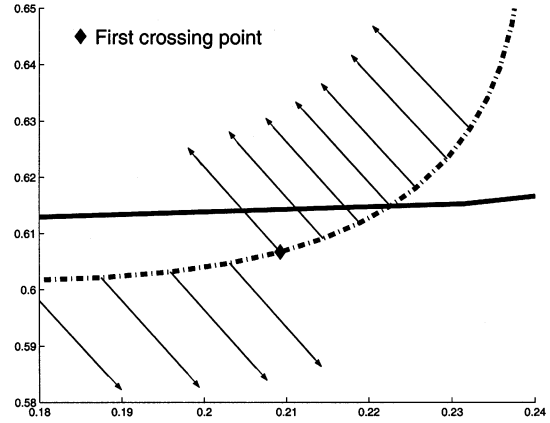

(b) First crossing

Figure 10. Eigenvectors along pinch-point curve for a reachable region with S-shaped distillation lines.

Numerical methods to detect the extended reachable region

In developing a feasibility test, we need to construct the true reachable region by taking into account the additional area resulting from S-shaped distillation lines. The first reflux (or reboil) ratio for which a sectional profile crosses the pinch-point curve marks the beginning of the extended reachable region. The other endpoint for the extended region is a point along the distillation line at which all sectional profiles have reentered the traditional reachability bounds. These points are depicted in Figure 8 for a stripping section. For the specified bottoms product, any stripping section with a reboil ratio of at least 1.97 will operate outside the minimum and total reflux bounds if enough stages are used.

There are two techniques that can be used to detect the point where profiles begin crossing the pinch-point curve. The first method computes the angle between the mass-balance line and the phase-equilibrium step for each stage along a sectional profile, as shown in Figure 9a for the acetone–chloroform–methanol mixture. When the sectional profile intersects the pinch-point curve, the angle is zero because the material balance and VLE step are colinear to the specified end-product composition. If the particular profile crosses the minimum reflux bound, the angle will switch signs after the crossing. This feature is shown for the same system in Figure 9b. The sign of the angle changes after the potential pinch point because the profile starts to approach the actual pinch point from the opposite direction. To use this technique effectively, sectional profiles for a range of reflux (or reboil) ratios would have to be searched, starting from a very low reflux (or reboil) up until a sign change is found. The reflux (or reboil) ratio associated with the profile where a sign change in the angle is first detected marks the beginning of the extended reachable region.

A more computationally efficient algorithm for locating the first cross point is based on the eigenvalue analysis developed by Pöllmann and Blass (1994). In this method, a linear approximation to sequential stage to stage calculations is used to study how sectional profiles approach a pinch point ($\boldsymbol{x}_p$).

For the stripping section, the linearization is

$$\boldsymbol{x}_n = \boldsymbol{x}_p + \sum_{i=1}^{NC-1} c_i \lambda_i^n \boldsymbol{\nu}_i \tag{1}$$

The eigenvalues (λ_i) and eigenvectors ($\boldsymbol{\nu}_i$) are determined from the Jacobian matrix ($\underline{\boldsymbol{J}}$) along the pinch-point curve

$$\underline{\boldsymbol{J}} = \frac{\delta \boldsymbol{x}_{n+1}}{\delta \boldsymbol{x}_n} \tag{2}$$

The computed eigenvectors are used to determine the direction in which sectional profiles approach pinch points. Figure 10a illustrates the eigenvectors for a stripping section in the acetone–chloroform–methanol mixture. Starting from the specified bottoms product, eigenvectors initially point away from the traditional reachable region. This indicates that profiles move from within the reachable region toward the pinch point. When the pinch-point curve is first crossed, the eigenvectors switch direction and point back toward the traditional reachable region, as shown in Figure 10b. Eigenvectors continue to point back into the enclosed area until sectional profiles enter the next enclosed area. From this point onward, eigenvectors behave the same as they do in the first reachable area and point away from the closed region. The direction of the eigenvector shows how a column section profile approaches a pinch point. When the direction changes from one side of the pinch point curve to the other, sectional profiles must cross through the pinch-point curve and come back from the other side. By locating the pinch point where eigenvectors switch direction, the beginning of the extended region and the corresponding reflux (or reboil) ratio giving rise to crossing profiles are found.

From looking at the crossing profiles in Figure 5, sectional profiles drawn at higher reboil ratios later cross into the second reachable region along the distillation line. Hence, the other endpoint for the extended reachable region can be found by drawing a profile at a high reflux (or reboil) ratio and determining the stage along the distillation line where the profile reenters.

Having located the first crossing point and the point where all profiles have returned to the traditional bounds, we next find the bound on the extended region. Since we have yet to identify a rigorous condition that gives the outer bound on the extended region, we use a convex-hull strategy to approximate the additional reachable area. The difficulties with precisely tracking the bound on the extended region are summarized in Appendix A. To approximate the region, a number of crossing sectional profiles are drawn, from which the convex hull of the reachable region is found. If enough sectional profiles are used, this method will provide an accurate bound. Figure 11 illustrates an extended region found using the convex-hull technique. As shown, the extended region is significant and should not be neglected. When compared to the first region of traditional reachability, the extended region adds 18% of additional reachable area for the acetone–chloroform–methanol system. This amounts to approximately 3% of the total reachable area.

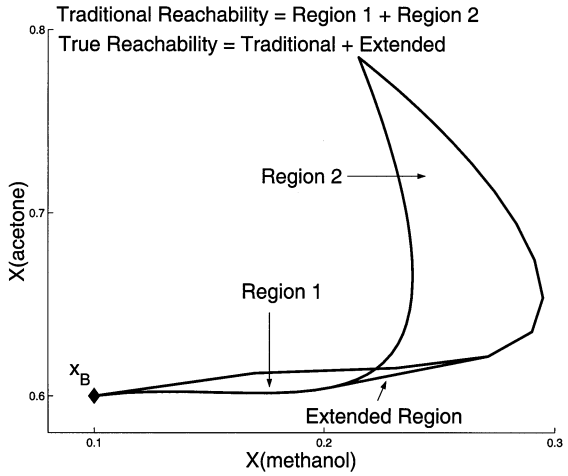

Figure 11. Traditional vs. extended reachability.

Feasibility Analysis and Column Design with S-shaped Total Reflux Curves

A procedure will be developed now to identify feasible regions for column sections separating nonideal ternary mixtures. Once reachable regions are found for the rectifying and stripping sections with specified end-products, the full column producing both products can be immediately checked for feasibility and suitable operating conditions can be identified. This method builds on the design algorithm of Castillo (1998) by accounting for the possibility of S-shaped total reflux curves. We will assume the full column operates with fixed pressure, constant molar overflow, equilibrium stages, and a single feed. The method is as follows:

Step 1. Specify Column Pressure, Distillate Composition ($\boldsymbol{x}_D$), and Bottoms Composition ($\boldsymbol{x}_B$).

Step 2. Construct Total Reflux Bounds from $\boldsymbol{x}_D$ and $\boldsymbol{x}_B$.

Step 3. Construct Minimum Reflux Bounds from $\boldsymbol{x}_D$ and $\boldsymbol{x}_B$.

Step 4. Check for S-Shaped Total Reflux Curves. To determine if S-shaped total reflux curves are present, the unidistribution and univolatility lines are first constructed using the VLE relationship. The total reflux curves through both end-products must be checked for inflection points by applying the two conditions described earlier. When an inflection point exists, a convex-hull approach can be used to approximate the extended reachable region.

Step 5. Check for Full Column Feasibility. If the feasible regions, including any extended regions resulting from S-shaped total reflux curves, for the two column sections overlap, then the full column is feasible and both end-products can be produced simultaneously from the same column. Otherwise, the specifications in step 1 need to be adjusted until overlapping feasible regions are found.

Step 6. Identify Suitable Operating Conditions. With feasibility established, the focus now shifts to finding operating conditions that best satisfy the design objectives. The key requirement is that the profiles for the rectifying and stripping sections intersect as described by Julka and Doherty (1990). To accomplish this, both sectional profiles must have a suitable reflux (or reboil) ratio to move into the overlapped reachable region. The sum of the number of stages along each sectional profile gives the total number of equilibrium stages

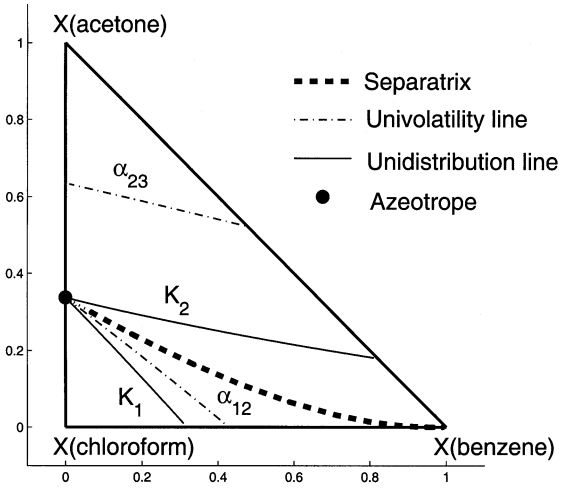

Figure 12. VLE features for Example 1.

in the column. An overall column balance can then be used to determine the feed composition, feed quality, and relative flow rates (D/F and B/F).

Implications of S-shaped total reflux curves

We have shown how the presence of S-shaped distillation lines allows column sections to operate beyond the minimum and total reflux bounds. We now apply the feasibility algorithm and find column designs that produce a specified distillate and bottoms product by taking advantage of the extended reachable region. The following examples illustrate the opportunities made possible by S-shaped total reflux curves.

Example 1: acetone – chloroform – benzene

The first example investigates the acetone–chloroform–benzene mixture shown in Figure 12. This ternary system has a distillation boundary joining the acetone–chloroform binary azeotrope (338 K) with pure benzene (353 K). Distillation lines in the upper region begin at acetone (329 K) and terminate at benzene, while total reflux curves head from chloroform (334 K) to benzene in the lower region. According to the two conditions for detecting S-shaped total reflux curves, there are two regions where inflection points are present—above the α_{23} univolatility line and to the right of the $\alpha_{12} = 1$ line.

For a distillate product in the upper distillation region, the traditional feasibility bounds for a staged rectifying section are constructed in Figure 13. Since the distillation line and pinch-point curve intersect at three points, an extended region exists. This is expected, since $\boldsymbol{x}_D$ lies above the α_{23} univolatility line. A thorough analysis of this system reveals that an extended region exists between the two points marked on Figure 13. With enough stages, any column section profile with a reflux ratio greater than 2 will cross outside the traditional bounds. In terms of area, this additional region is 37% of the size of the first region and makes up 2% of the total reachable area from the specified end-product.

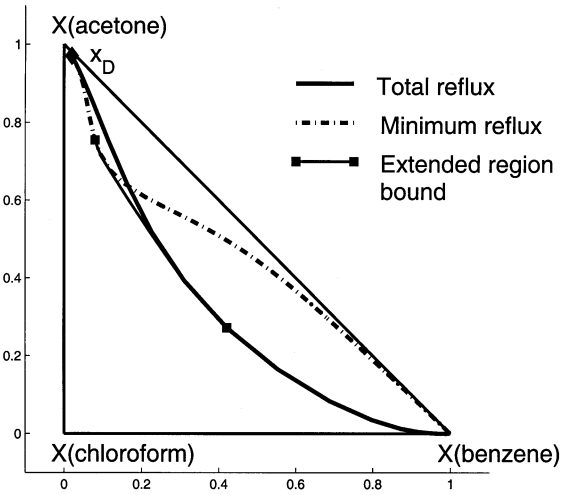

Figure 13. Feasible region for Example 1 with an S-shaped distillation line in the rectifying section bounds.

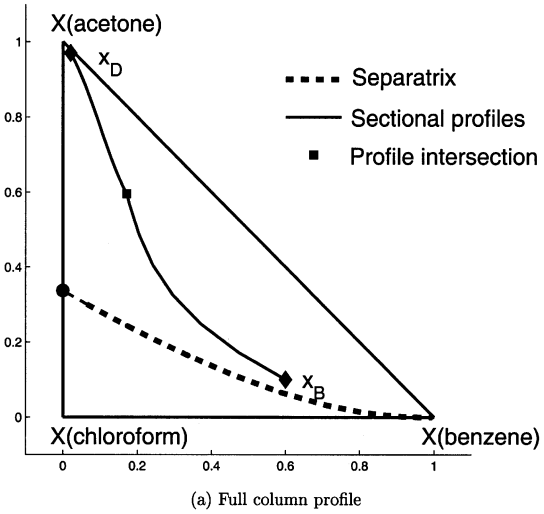

(a) Full column profile

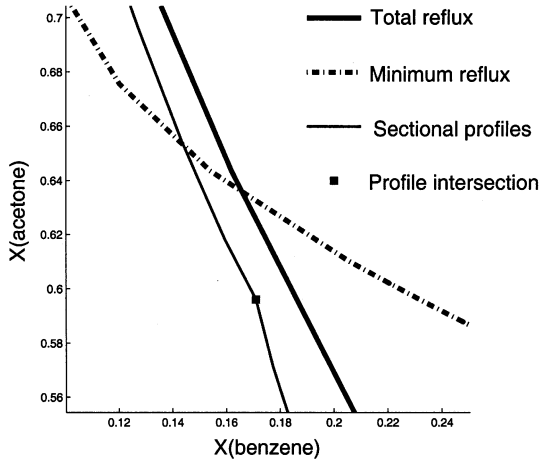

(b) Profiles intersect in extended region

Figure 14. Feasible column for Example 1 in extended region.

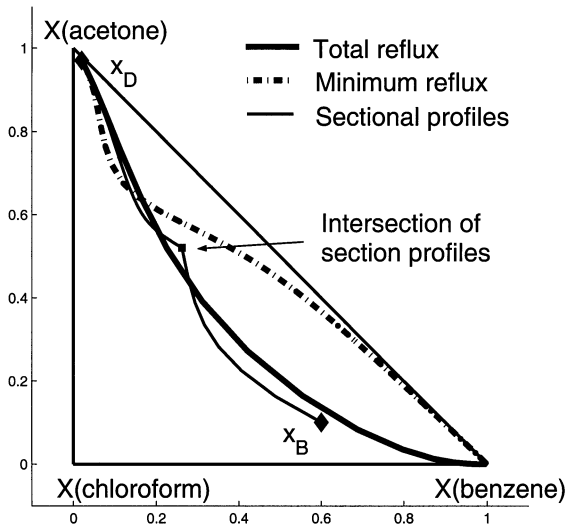

Figure 15. Feasible column for Example 1 in region beyond the extended region.

Using the distillate composition and the corresponding feasible region from Figure 13, a full column design with the rectifying and stripping profiles intersecting in the extended region is illustrated in Figure 14. The column has 18 stages, 10 rectifying and 8 stripping, and operates at a reflux ratio of 3 and a reboil ratio of 15. This separation is feasible because the profiles intersect, which means a feed can be found that will split into the desired products. Columns can also operate in the enclosed area beyond the extended region. The rectifying profile in Figure 15 uses 23 stages and a reflux ratio of 2.5 to pass through the extended region and then intersect the stripping profile with 9 stages and a reboil ratio of 5 in the lower enclosed area.

Example 2: acetic anhydride – water – acetic acid

The next example is a mixture of acetic anhydride, water, and acetic acid that has a separatrix connecting the acetic anhydride–water azeotrope (363 K) with the acetic anhydride–acetic acid azeotrope (383 K), as shown in Figure 16a. Total reflux curves terminate at acetic anhydride (412 K) in the upper region and at acetic acid (391 K) in the lower region. This system will be used to illustrate how packed columns described by differential profiles can also operate in extended regions of composition space due to S-shaped residue curves. For a distillate product placed close to the separatrix, the reachable feeds for a rectifying section are represented in Figure 16a. The residue curve through $\boldsymbol{x}_D$ intersects the pinch-point curve at three points, leading to an extended reachable region. If a desired bottoms product is now specified near pure acetic acid, the region of reachable feeds for a stripping section can be determined, as done in Figure 16b. The traditional bounds for the stripping section only intersect at two points, resulting in no extended region. By comparing the reachable compositions for both column sections, we see that the two feasible regions overlap. This indicates that a feasible full column design can be found that

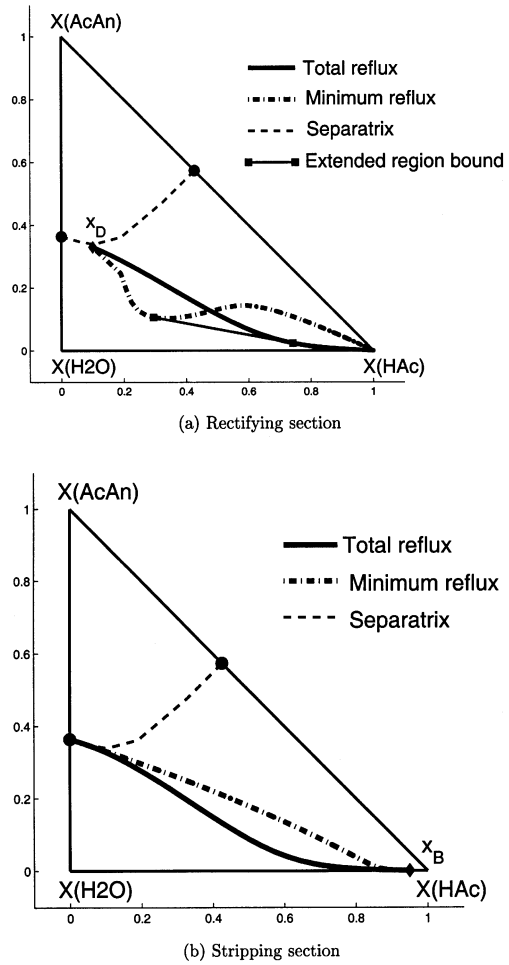

Figure 16. Reachable feeds for Example 2.

produces both $\boldsymbol{x}_D$ and $\boldsymbol{x}_B$. One feasible full column design is shown in Figure 17. The sectional profiles for this design take advantage of the S-shaped residue curves and intersect in the extended region of reachable feeds for the rectifying section. The column operates at a reflux ratio of 1.5 and a reboil ratio of 8.

Conclusions

This article has identified and verified the presence of an extended reachable region for mixtures with S-shaped distillation lines. We have presented a method to quickly determine if S-shapes are possible. We have also shown how to locate and bound the extended reachable region for a column section. Together, these methods form a powerful tool to test the feasibility of distillation schemes for nonideal mixtures.

The actual size of the extended reachable region is relatively small compared to that found from traditional reachability. However, the fact that this additional region exists is important from a process synthesis perspective. The true reachable region must be known if it is to be used as a complete criterion for determining column section feasibility. Otherwise, viable process alternatives could be ruled out, inadvertently leading to a suboptimal design.

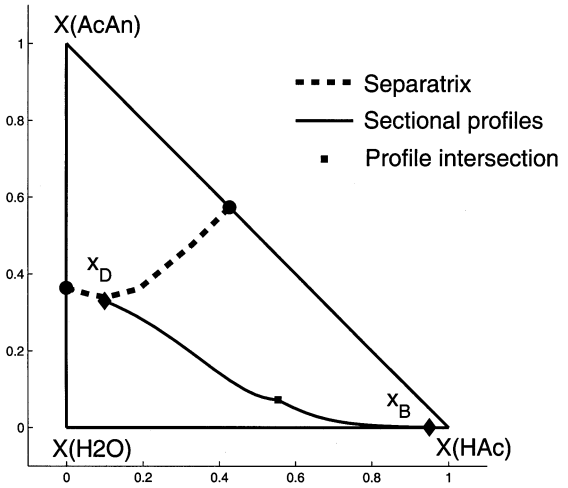

Figure 17. Feasible column for Example 2 in extended region.

Although S-shaped distillation lines increase reachability for distillation, the opportunities may be more profound when combined with a chemical reaction. The product composition region for an arbitrary combination of reactive and nonreactive sections is today primarily found by the trial-and-error approach. Unless the principles behind extreme and optimal section profiles can be identified and understood, the design task may readily become computationally prohibitive or limited to a restrictive subset of structural alternatives.

Acknowledgment

The authors thank Professor Arthur W. Westerberg (Carnegie Mellon) for his contributions in the early stages of this work.

Notation

$A_{i,j}$ = binary interaction parameter in Wilson model, $J \cdot mol^{-1}$
B = bottoms product flow rate (amount/time)
C_i = parameter in Wagner vapor-pressure equation
D = distillate product flow rate (amount/time)
F = feed flow rate (amount/time)
$\Delta G_{i,j}$ = binary interaction parameter in NRTL model, $J \cdot mol^{-1}$
$\underline{J}$ = Jacobian matrix
K = distribution coefficient, $K_i = y_i/x_i$
NC = number of components
P_c = critical pressure, kPa
T_c = critical temperature, K
$a_{i,j}$ = binary interaction parameter in NRTL model
r = reflux ratio
s = reboil ratio
$\boldsymbol{x}$ = liquid-phase mole fraction
$\boldsymbol{y}$ = vapor-phase mole fraction

Greek letters

$\alpha_{i,j}$ = relative volatility, $\alpha_{i,j} = (y_i/x_i)/(y_j/x_j)$
λ_i = eigenvalue of $\underline{J}$
$\boldsymbol{\nu}_i$ = eigenvector of $\underline{J}$
θ = angle between equilibrium step and mass-balance line

Subscripts and superscripts

B = subscript for bottoms product
D = subscript for distillate product
n = subscript when leaving stage n
p = subscript for pinch point
n = superscript for stage number

Literature Cited

Castillo, F., D. Thong, and G. Towler, "Homogeneous Azeotropic Distillation: 1. Design Procedure for Single-Feed Column at Nontotal Reflux," *Int. Eng. Chem. Res.*, **37**, 987 (1998).
Doedel, E., "Auto 97: Continuation and Bifurcation Software for Ordinary Differential Equations," http://indy.cs.concordia.ca/auto (1998).
Doherty, M., and J. Perkins, "On the Dynamics of Distillation Processes: I. The Simple Distillation of Multicomponent Non-Reacting, Homogeneous Liquid Mixtures," *Chem. Eng. Sci.*, **33**, 281 (1978).
Fidkowski, Z., M. Doherty, and M. Malone, "Feasibility of Separation for Distillation of Non-Ideal Ternary Mixtures," *AIChE J.*, **39**, 1303 (1993).
Giessler, S., R. Danilov, R. Pisarenko, L. Serafimov, S. Hasebe, and I. Hashimoto, "Feasible Separation Modes for Various Reactive Distillation Systems," *Ind. Eng. Chem. Res.*, **38**, 4060 (1999).
Hilmen, E., "Separation of Azeotropic Mixtures: Tools for Analysis and Studies on Batch Distillation Operation," PhD Thesis, Norwegian Univ. of Science and Technology, Trondheim (2000).
Julka, V., and M. Doherty, "Geometric Behaviour and Minimum Flows for Nonideal Multicomponent Distillation," *Chem. Eng. Sci.*, **45**, 1801 (1990).
Kiva, V., and L. Serafimov, "Rules that Govern the Composition Trajectories of Simple Distillation of Ternary Mixtures," *Russ. J. Phys. Chem.*, **47**, 638 (1973).
Pöllmann, P., and E. Blass, "Best Products of Homogeneous Azeotropic Distillation," *Gas Sep. Purif.*, **8**, 194 (1994).
Serafimov, L., "Thermodynamic Topological Analysis and the Separation of Multicomponent Polyazeotropic Mixtures," *Theor. Found. Chem. Eng.*, **21**, 44 (1987).
Stichlmair, J., "Distillation and Rectification," *Ullmann's Encycl. Ind. Chem.*, **B3**, pp. 4-1/4-94 (1988).
Van Dongen, D., "Distillation of Azeotropic Mixtures: The Application of Simple-Distillation Theory to Design of Continuous Processes," PhD Thesis, Univ. of Massachusetts, Amherst (1983).
Wahnschafft, O., "Synthesis of Separation Systems for Azeotropic Mixtures With an Emphasis on Distillation-Based Methods," PhD Thesis, Technical Univ. of Munich, Munich (1992).
Wahnschafft, O., J. Koehler, E. Blass, and A. Westerberg, "The Product Composition Regions of Single Feed Azeotropic Distillation Columns," *Ind. Eng. Chem. Res.*, **21**, 2345 (1992).
Westerberg, A., and O. Wahnschafft, "Synthesis of Distillation-Based Separation Systems," *Adv. Chem. Eng.*, **23**, 63 (1996).

Appendix A: Convex-Hull Approximation

The extended reachable region resulting from S-shaped total reflux curves is bounded using a convex-hull approach. This approximation technique overcomes a number of difficulties encountered when trying to find an exact bound on the feasible region.

The bound on the additional reachable region shares several characteristics with the pinch-point curve. We know that the bound is parametric in the reflux ratio. We have shown that once the first crossing point is located, all higher reflux ratios lead to profiles heading into the extended region. Another similarity between the two bounds is that each point on the bound belongs to a different sectional profile. On a mini-

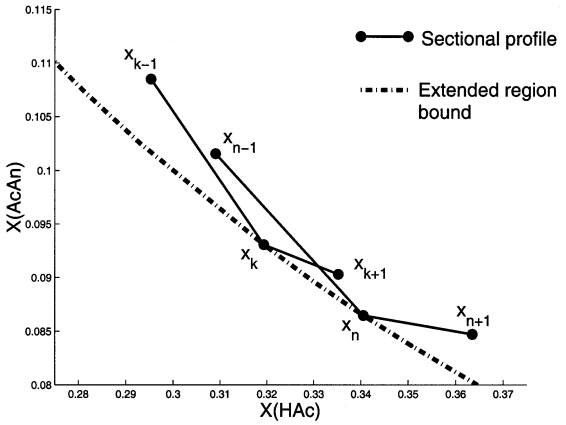

Figure A1. Sectional profiles touching the bound on the extended reachable region.

Table A1. Wilson Activity Coefficient Parameters

Component i	Component j	$A_{i,j}$ [J·mol^{-1}]	$A_{j,i}$ [J·mol^{-1}]
Acetone	Benzene	2,288.7	−906.29
Acetone	Chloroform	485.83	−2,120.7
Acetone	Methanol	−660.99	2,479.6
Benzene	Chloroform	621.07	−872.36
Chloroform	Methanol	−1,513.7	7,087.8

mum reflux curve, each point along the curve is a termination point for a column section profile drawn at a different reflux. In Figure A1, two sectional profiles are shown for the acetic anhydride–water–acetic acid system. The profile with stage index k has a reflux of 0.6, while the profile with index n has a reflux of 0.7. Both profiles touch a unique point along the true extended region bound.

However, there is one key difference between the pinch-point curve and the bound on the extended region that complicates matters. The pinch-point curve has a geometric description—each point is colinear with the equilibrium vapor composition and the end-product. This colinearity condition eliminates the issue of sectional profile path dependency and allows the curve to be tracked directly without computing any sectional profiles. For the extended region bound, we have yet to determine a geometric condition that holds for each point along the bound. We are uncertain if such a condition actually exists. Even when one point on the bound is known, there is no way to determine where the next point will lie for a small perturbation in reflux. This can be seen in Figure A1. If a point on the true bound such as $\boldsymbol{x}_k$ is known, there is no obvious relationship between $\boldsymbol{x}_{n-1}$, $\boldsymbol{x}_n$, or $\boldsymbol{x}_{n+1}$ because these points lie on a completely different sectional profile. This path dependency is a consequence of the alternating material balance and phase equilibrium steps used to compute sectional profiles.

Due to the path dependency, we have used a convex hull to approximate the bound on the extended region. The method proceeds by finding the first crossing point using the eigenvectors drawn for each pinch point. We then take a range of reflux ratios, starting from the reflux marking the start of the extended region. For each reflux ratio, the sectional profile is computed until it pinches. Then a convex hull of the traditional reachable bounds and the computed profile is found to make sure the part of the sectional profile in the extended region is captured. If this is repeated for a large range of reflux ratios, the convex hull will closely approximate the exact bound.

While the traditional feasibility bounds can be computed using geometric conditions without the need to draw a single sectional profile, the convex-hull technique requires a number of profiles to be computed at finite reflux. This method

Table A2. Wagner Vapor-Pressure Parameters

Component	C_1	C_2	C_3	C_4	P_c [kPa]	T_c [K]
Acetone	−7.45514	1.20200	−2.43926	−3.35590	4,700	508.1
Benzene	−6.98273	1.33213	−2.62863	−3.33399	4,890	562.2
Chloroform	−6.95546	1.16625	−2.13970	−3.44421	5,370	536.4
Methanol	−8.54796	0.76982	−3.10850	1.54481	8,090	512.6

Table A4. Antoine Vapor-Pressure Parameters

Component	A	B	C
Acetic anhydride	14.385	3,287.6	−52.360
Water	16.285	3,816.4	−46.130
Acetic acid	14.795	3,405.6	−56.340

Table A5. System Specifications

Figure Nos.	System	Specifications
1	*	$\boldsymbol{x}_B = [0.10\ 0.30\ 0.60]$
5,8,9,10,11	**	$\boldsymbol{x}_B = [0.60\ 0.30\ 0.10]$
13	*	$\boldsymbol{x}_D = [0.97\ 0.01\ 0.02]$
14	*	$\boldsymbol{x}_D = [0.97\ 0.01\ 0.02]$ $\boldsymbol{x}_B = [0.10\ 0.30\ 0.60]$ $r = 3\ s = 15$
15	*	$\boldsymbol{x}_D = [0.97\ 0.01\ 0.02]$ $\boldsymbol{x}_B = [0.10\ 0.30\ 0.60]$ $r = 2.5\ s = 5.0$
16,17	†	$\boldsymbol{x}_D = [0.330\ 0.570\ 0.100]$ $\boldsymbol{x}_B = [0.001\ 0.049\ 0.950]$ $r = 1.5\ s = 8.0$
A1	†	$\boldsymbol{x}_D = [0.33\ 0.57\ 0.10]$

*Acetone–chloroform–benzene.
**Acetone–chloroform–methanol.
†Acetic anhydride–water–acetic acid.

Table A3. NRTL Activity-Coefficient Parameters

Component i	Component j	$\Delta G_{i,j}$ [J·mol^{-1}]	$\Delta G_{j,i}$ [J·mol^{-1}]	$a_{i,j}$
Acetic anhydride	Water	2,652.3	2,102.8	−0.91
Acetic anhydride	Acetic acid	2,351.6	179.92	0.30
Acetic acid	Water	−3,330.4	5,174.7	0.10

significantly slows down the task of identifying feasibility bounds, but it provides a close approximation of the true bound, which is the key to synthesizing alternative distillation schemes based on feasible regions.

Appendix B: Thermodynamic Data and System Specifications

The thermodynamic calculations for the acetone–chloroform–methanol and acetone–chloroform–benzene mixtures used throughout this study are based on the Wilson model for liquid activity coefficients and the Wagner equation for vapor pressure. The parameters for these correlations are presented in Tables A1 and A2 (Pöllmann and Blass, 1994). Vapor–liquid equilibrium calculations for the acetic anhydride, water, and acetic acid mixture are performed using the NRTL activity coefficient model along with Antoine's vapor-pressure equation. The parameters are taken from Giessler et al. (1999) and listed in Tables A3 and A4. Product specifications and column operating parameters for the systems studied in this article are given in Table A5. The pressure for all separations is 101.3 kPa.

Manuscript received Feb. 19, 2001, and revision received May 20, 2002.